Muon reactivation in muon-catalyzed d-t fusion from accurate p-He^+ stripping and excitation cross sections

C. D. Stodden and H. J. Monkhorst
Quantum Theory Project, Department of Physics, University of Florida, Gainesville, Florida 32611

K. Szalewicz
Department of Physics, University of Delaware, Newark, Delaware 19716

T. G. Winter
Department of Physics, Pennsylvania State University, Wilkes-Barre Campus, Lehman, Pennsylvania 18627

(Received 20 July 1989)

Accurate cross sections are obtained for the excitation and stripping of a muon from $\alpha\mu$ in collisions with hydrogen atoms. This is done by calculating the excitation, ionization, and charge-transfer cross sections for the p-He^+ collision and scaling the results. An impact-parameter coupled-state method with a basis set of up to 51 Sturmian wave functions is used to obtain cross sections at center-of-mass energies ranging from 20 to 600 keV. Along with Stark, Auger, radiative, and stopping rates these cross sections are used to calculate the probability of stripping a muon from $\alpha\mu$ by numerically solving a set of coupled differential equations that describe the kinetics of $\alpha\mu$ as it travels through a mixture of D_2 and T_2. An effort has been made to minimize the uncertainty in the value of the stripping probability resulting in error bars of 9% and 11% at densities of 1.2 and 0.05 times liquid-hydrogen density, respectively. X-ray yields belonging to K and L series transitions among $\alpha\mu$ states have also been computed. The present results are compared with recent theoretical and experimental data.

I. INTRODUCTION

The process of using a muon (μ) to repeatedly induce the fusion of hydrogen isotopes at thermal energies is known as muon-catalyzed fusion (MCF). The efficiency of MCF is determined by the number of fusion events per muon during its lifetime. It is limited by the fraction of muons which are lost to the catalytic cycle via "sticking" to the α particle which is created in the fusion process. The muon is lost only if it remains "stuck" to α for its entire lifetime. If the muon is stripped by collisional ionization or charge transfer with the surrounding hydrogen isotopes, it is returned to the fusion cycle, thereby adding to the efficiency of MCF.

Among the several fusion reactions which muons can catalyze, t-d fusion is the most promising due to the largest formation rate of $td\mu$. The muon sticking to the α particle appears now to be the major bottleneck of this MCF cycle. The probability that a muon will stick to the α particle after a fusion event, and remain stuck to it even after slowing down, is known as the effective sticking fraction w_s^{eff}. Despite much effort spent in investigating sticking there exists a substantial discrepancy between theory and experiment in the value of the effective sticking fraction. For a D_2-T_2 mixture at 1.2 times liquid-hydrogen density (LHD) the average of recent experimental results [Jones *et al.*,[1] (0.35±0.07)% (the ±0.07% estimate is from private communications); Breunlich *et al.*,[2] (0.45±0.05)%; Nagamine *et al.*,[3] (0.46±0.07)%; Bossy *et al.*,[4] (0.42±0.14)%] for w_s^{eff} is (0.42±0.09)%. At the same time recent theoretical works all arrive at sticking of between 0.57% and 0.58% (Refs. 5–7) at this density which is outside of the experimental value by about two standard deviations. The error of the theoretical value was estimated to be about ±0.05%. Thus the error bars of the experimental and theoretical values do not overlap. In addition experiments by Jones *et al.* and by Breunlich *et al.* resulted in drastically different dependences of sticking on density. Theoretical density dependence agrees reasonably well with the latter measurement. Since the sticking fraction sets limits on the effectiveness of MCF, further investigation of this quantity appears to be a vital task in MCF research.

The probability that the muon will be stripped from the α particle is known as the reactivation coefficient, and is denoted by R. The value of R has been studied by many authors using various theoretical methods to calculate cross sections and various models for the dynamical processes involved. The first discussion of the reactivation process is found in Jackson's classic paper of 1957.[8] A value for R of 22% was calculated by Jackson using a method which employed experimental values from electron loss cross sections for (αe)-H_2 scaled to the $\alpha\mu$ system to obtain stripping cross sections, which were then extrapolated to very high velocities using a v^{-2} behavior where v is the velocity of $\alpha\mu$. The value for R obtained by Jackson was independent of density because in the dynamical model used the muon was stripped from α in a one step process. This model was also used by Gershtein *et al.* in their paper of 1981.[9] Using more appropriate

experimental values for the stripping cross section their resulting value for R was 23%, nearly identical to Jackson's. A great improvement in the value of R was made in a paper by Bracci and Fiorentini[10] in which scaled experimental values were again used for stripping, but a classical trajectory Monte Carlo (CTMC) calculation was used to extrapolate to very high velocities ($v > 4.4$ a.u.). In addition the Born approximation was used to calculate excitation cross sections to electronically excited states and CTMC to calculate stripping cross sections from these excited states. These cross sections were used in a model of reactivation which now involved a multiple step process whereby the muon was allowed to undergo several transitions before being stripped. In this multistep model the value of R is density dependent and was calculated to be 24% at a density equal to that of liquid hydrogen. There have been other calculations of R since then which also use the multiple step model, each using slightly different methods for one or more of the cross sections and some including more transitions than others.[5-7,11-14] For example, at about one liquid hydrogen density (1 LHD) R is calculated to be 32% by Men'shikov and Ponomarev,[11] 25% by Takahashi,[12] 35% by Markushin,[6] 35% by Struensee and Cohen,[14] and 36% by Rafelski *et al.*[7]

The process of stripping the muon from $\alpha\mu$ is directly analogous to the following proton-hydrogenic-ion reactions,

$$\mathrm{He}^+ + \mathrm{H}^+ \rightarrow \begin{cases} \mathrm{He}^{2+} + \mathrm{H}^+ + e^- \quad \text{(ionization)} & (1) \\ \mathrm{He}^{2+} + \mathrm{H} \quad \text{(charge transfer)} & (2) \end{cases}$$

One electron processes such as these are interesting in themselves and have been studied extensively both theoretically and experimentally.[15-32] The most accurate stripping calculations to date use experimental data to obtain cross sections for Eqs. (1) and (2) and scale them to the muonic system.[6,7,14] These experimental data typically have error bars of about ±20% which are passed on to the calculation of R. This results in error bars for R between ±14% and ±17% depending on the density of the surrounding hydrogen isotope mixture. The error bars in the reactivation coefficient R can be narrowed by computing accurately the important cross sections such as those for Eqs. (1) and (2). The purpose of the present work is to provide cross sections for the proton-He^+ system from extensive calculations and after scaling them to the muonic system, use in the calculation of R within the multiple step model of reactivation.

By far the most important quantities affecting the stripping process of $\alpha\mu$ are the ionization and charge transfer cross sections from the $1s$ state and the stopping cross section of $\alpha\mu$ in the hydrogen isotope mixture. The stopping cross section as a function of velocity is assumed to be equal to that for protons in hydrogen which is available in tables compiled from several different experiments.[33] Presently this is the best way to obtain stopping cross sections and we will not attempt to reduce the error bars on these values. However, it is important to note that the error introduced into the value of R by the uncertainty in the stopping cross section is only about ±5% at liquid hydrogen density (LHD) while the experimental stripping (ionization plus charge transfer) cross sections introduce about ±15% uncertainty at LHD.

The stripping of $\alpha\mu$ at LHD is a multistep process involving not only direct stripping from the ground state but also excitation and deexcitation between $\alpha\mu$ states and stripping from excited $\alpha\mu$ states. Inclusion of such processes can increase the value of R by about 25%. The most important of these additional processes are the excitation to and stripping from states with $n=2$ and $n=3$. The present calculations provide accurate cross sections for $1s$-$2s$, $1s$-$2p$, $1s$-$3s$, $1s$-$3p$, and $1s$-$3d$ excitations in addition to stripping and charge transfer cross sections from the $1s$ state.

These calculations are based on an impact-parameter, coupled-states formalism in which the nuclei are treated classically and the electron (muon), quantum mechanically. The wave function for the electron is expanded in a two-center Sturmian pseudostate basis set, where one center is the target α and the other the projectile p. These calculations have been carried out previously by Winter with smaller basis sets.[22-24] By using a very large basis set of 51 functions we will be able to check the convergence of the previous stripping results, extend these to higher energies, and provide accurate excitation cross sections.

The main purpose of the present work is to calculate the reactivation coefficient. However, because there is interest in cross sections for the p-He^+ system apart from the application to MCF we will present a brief overview of the coupled-state Sturmian method in Sec. II and present diagnostics and results for the proton-He^+ system in Sec. III. In Sec. IV we will review the kinetics of stripping in MCF and use the cross sections from Sec. III in the kinetic equations to calculate the reactivation coefficient R.

II. METHOD

Several theoretical methods have been used to calculate cross sections for collisional ionization and charge transfer between two atoms. In choosing the method best suited for a particular problem one must consider the kinetic energies involved and the desired accuracy. The first Born approximation for ionization is best suited for very high center-of-mass collision energies (>400 keV). For high accuracy at very low collision energies (<1 keV) a proper approach would be some type of time-independent coupled channels method in which the nuclei and electron are all treated quantum mechanically. For intermediate energies (~1 to 600 keV) one may simplify this approach to a time-dependent coupled states method in which the nuclei are treated classically and the electron quantum mechanically.[34] In this method the wave function for the electron may be expanded in various basis sets (molecular, atomic, pseudostate, etc.) depending again on the energies and the system involved.

We have chosen a time-dependent, coupled-states method which uses Sturmian functions centered on each nucleus to expand the electronic wave function. The

method was first applied by Wilets and Gallaher[15] to the proton-hydrogen electron transfer process; it was further developed and tested with a larger basis by Shakeshaft.[16,17] Winter applied the method to the proton-helium ion system using even larger bases (up to 35 functions),[22–24] and obtained excellent agreement with experimental results for total electron stripping at energies from 14 to 120 keV center-of-mass energies. More recently Winter[25] has obtained cross sections for a three-center expansion on the same system and extended them to even lower energies. The present study uses Winter's two-center method with 51 (and 43) functions to obtain stripping as well as excitation cross sections for the $He^+(1s)+H^+$ system.

The details of the method can be found in a paper by Winter.[22] We will only briefly present the main points of the formalism here. In the time-dependent, coupled-states method the nuclei are assumed to move on a classical path, and the electrons satisfy a time-dependent Schrödinger equation. In the present study the so-called impact-parameter method was used in which the nuclei are assumed to move along straight lines with constant velocity such that $\mathbf{R}(t)=\mathbf{b}+\mathbf{v}t$, where $\mathbf{v}$ is the internuclear velocity, $\mathbf{b}$ is a vector perpendicular to $\mathbf{v}$ with length equal to the impact parameter, and $\mathbf{R}$ is the coordinate of nucleus B relative to nucleus A in a collision between projectile A and target B. The wave function Φ for the electron satisfies the following time-dependent Schrödinger equation:

$$h\Phi=i\hbar\frac{\partial\Phi}{\partial t} . \tag{3}$$

For a simple one-electron system (neglecting spin-orbit coupling) the Hamiltonian h is

$$h(t)=-\frac{\hbar^2}{2m}\nabla^2-\frac{Z_Ae^2}{r_A}-\frac{Z_Be^2}{r_B}+\frac{Z_AZ_Be^2}{R} , \tag{4}$$

where the gradient contains the derivative with respect to any inertial frame, m is the reduced mass of the electron-nucleus system, and r_α ($\alpha=A,B$) denotes the position of the electron with respect to nucleus α. The inertial frame of reference chosen to define the gradient is centered at the midpoint between A and B. We will define the vector $\mathbf{r}'$ to be the position vector of the electron in this reference frame. The time derivative in Eq. (3) must be taken holding $\mathbf{r}'$ fixed, therefore $\partial/\partial t=(\partial/\partial t)_{r'}$. The internuclear potential energy term $Z_AZ_Be^2/R$ does not affect the results and can be neglected.

In order to solve Eq. (3) the electronic wave function is expanded in essentially two approximate atomic orbital basis sets, one centered on each nuclei, with time-dependent coefficients,

$$\Phi(\mathbf{r}',t)=\sum_\alpha\sum_k a_{k\alpha}(t)f_{k\alpha}(\mathbf{r}',t) , \tag{5}$$

where

$$f_{k\alpha}(\mathbf{r}',t)=\psi_{k\alpha}(\mathbf{r}_\alpha(\mathbf{r}',t))\exp\left[-iE_{k\alpha}t\mp i\frac{\mathbf{v}\cdot\mathbf{r}'}{2}-i\frac{v^2t}{8}\right] \tag{6}$$

and $\psi_{k\alpha}$ is an approximate atomic orbital wave function centered on nucleus α with approximate eigenvalue $E_{k\alpha}$. The vector $\mathbf{r}_\alpha$ is the position vector of the electron in an inertial frame relative to nucleus α. The atomic orbital wave function $\psi_{k\alpha}$ is determined by diagonalizing the atomic Hamiltonian

$$H_\alpha=\frac{\hbar^2}{2m}\nabla^2-\frac{Z_\alpha e^2}{r_\alpha} \tag{7}$$

in a finite basis set of Sturmian wave functions $\phi_{j\alpha}(\mathbf{r})$, where $j=(nlm)$. Thus $\psi_{k\alpha}$ is obtained as an expansion with time-independent coefficients:

$$\psi_{k\alpha}=\sum_j C_{kj\alpha}\phi_{j\alpha}(\mathbf{r}_\alpha) . \tag{8}$$

The Sturmian basis set is simply a set of scaled hydrogenic functions $\{\phi_{nlm}\}$ which satisfy the equation (in atomic units)

$$\left[-\tfrac{1}{2}\nabla_r^2-\frac{\kappa_{nl}}{r}+\frac{1}{2}\frac{\kappa_{nl}^2}{n^2}\right]\phi_{nlm}(\mathbf{r})=0 , \tag{9}$$

where $0\le|m|\le l$ and $\kappa_{nl}=n/(l+1)$. Note that the hydrogen atom wave functions are obtained by setting $\kappa_{nl}=1$. The use of the Sturmian basis in the present application is advantageous in that it is a complete set spanning both the bound and continuum regions of space. Thus it is possible to deal with excitation, electron transfer, and ionization all with a set of discrete functions.

The time-dependent coefficient $a_{k\alpha}(t)$ in Eq. (5) is obtained by substituting the expansion for Φ into the time-dependent Schrödinger equation and left multiplying by $f_{k\alpha}^*$ resulting in a set of coupled differential equations. In the following calculations the electron is initially in the $1s$ state of atom B so an initial boundary condition is $a_{k\alpha}(-\infty)=\delta_{1sB,k\alpha}$. The probability for a transfer to any final state β is given by $P_{k\beta}(\rho)=|a_{k\beta}(\infty)|^2$, where $\beta=A,B$ and ρ is the impact parameter. The cross section for transfer to any final state $k\beta$ is obtained by integrating ρ times the probability $P_{k\beta}(\rho)$ over all (relevant) impact parameters:

$$\sigma(1sB\to k\beta)=2\pi\int_0^\infty\rho P_{k\beta}(\rho)d\rho . \tag{10}$$

Thus σ is calculated by integrating the coupled differential equations along many trajectories, each having a different impact parameter such that the approximation to the integral in Eq. (10) is

$$\sigma(1sB\to k\beta)\approx2\pi\sum_{\rho=0}^{\rho_{\max}}\rho P_{k\beta}(\rho)(\Delta\rho) , \tag{11}$$

where $P_{k\beta}(0)$ is finite and $\rho_{\max}$ is of the order of a few Bohr radii.

The stripping probability for a given impact parameter is defined by the following sum over final states:

$$P_{\rm st}=\sum_k{}' P_{kB}+\sum_j P_{jA} , \tag{12}$$

where the primed sum is over only those states embedded in the continuum, for which $E_{kB}\ge0$. The stripping cross

section is defined by a similar sum over partial cross sections,

$$\sigma_{\rm st}^{(1s)}=\sum_k{}' \sigma(1s\rightarrow kB)+\sum_j \sigma(1s\rightarrow jA)\ . \tag{13}$$

The first sum in Eq. (13) is equal to the ionization cross section $\sigma_i^{(1s)}$ and the second sum to the charge-transfer cross section.

The time-dependent coupled equations which arise in the coupled-states method have been integrated using Hamming's method started by a Runge-Kutta integration.[35] The truncation error limits for the integration are between 5×10^{-6} and 5×10^{-4}. The coupled equations were integrated over the interval $z=vt$ from $-100a_0$ to $1000a_0$.

The charge exchange matrix elements have been evaluated by double numerical integration over the prolate spheriodial coordinates λ and μ where

$$r_\beta=(\lambda\pm\mu)\frac{R}{2}\ , \tag{14}$$

$$\cos\theta_\beta=\frac{\lambda\mu\pm1}{\lambda\pm\mu}\ , \tag{15}$$

with r_η and R the magnitudes of the position vectors of the electron with respect to nucleus β and of the two nuclei relative to each other, respectively. The angle θ_β is the polar angle for the electron and the upper and lower signs correspond to $\beta=A,B$. The exchange coupling was assumed negligible for values of $|z|>40a_0$.

TABLE I. Convergence of the total electron probability $\sum P_{k\beta}$ and impact parameter ρ times stripping probability $P_{\rm st}$ as a function of the number of integration points for several center-of-mass energies at $\rho=0.75$ a.u. using a basis set of 43 Sturmian functions.

λ	μ	$E_{\rm c.m.}$ (keV)	$\sum P_{k\beta}$	$\rho P_{\rm st}$
16	20	40		0.1230
24	24			0.1230
16	20	120	1.000 58	0.074 43
24	24		0.999 96	0.074 76
32	32		1.000 00	0.074 73
24	24	160	0.999 63	0.055 46
32	32		0.999 98	0.055 63
32	80		0.999 99	0.055 63

III. COLLISIONAL STRIPPING AND EXCITATION RESULTS

Table I illustrates the convergence of the total electron probability and the kernel of the stripping cross section integral as the number of integration points is increased. It can be seen from this table that as the energy is increased the mesh of points must become increasingly more dense to attain the same degree of convergence in the stripping cross section and in the total electron probability. The other cross sections converge in a similar fashion.

In order to span the relevant velocity range for the reactivation process ($v^2=1$ to 34 a.u.) we have carried out Sturmian calculations at $v^2=1.0$, 1.5, 2.0, 3.0, 6.0, 8.0, 12.0, and 30 a.u. Many of these were chosen near the peak at $v^2=2.0$ a.u. in order to provide a well-defined peak shape and position.

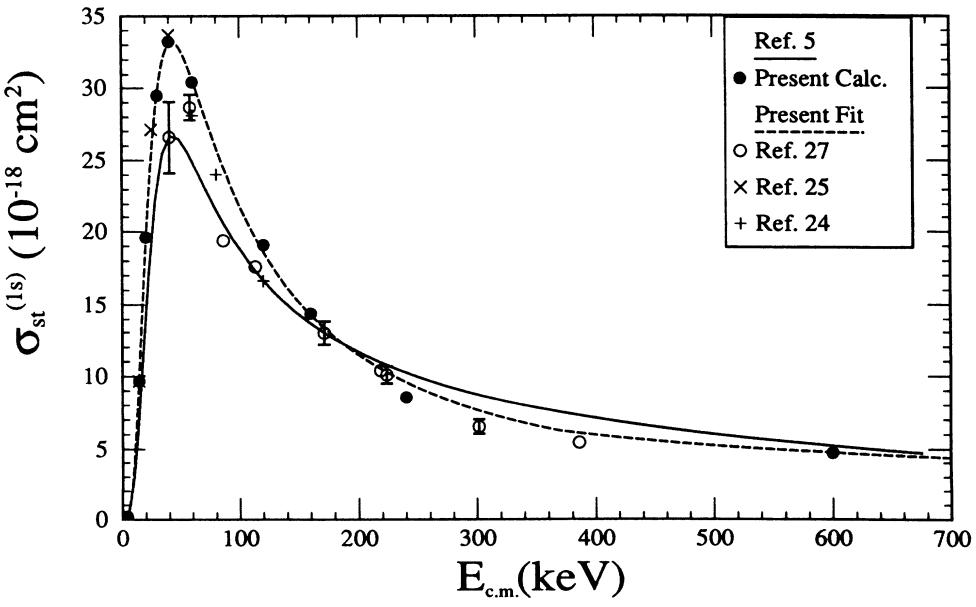

FIG. 1. Comparison of theoretical stripping cross sections for the p-He^+ system. The theoretical data plotted are from Cohen's fit of experimental data (Ref. 5), calculations by Winter using two-center (Ref. 24) and three-center (Ref. 25) basis sets, and the present calculations. The experimental data set plotted is from Angel *et al.* (Ref. 27) and is the only experimental data which includes energies greater than 200 keV.

TABLE II. Cross sections for collisions between protons and He^+ vs square of velocity.

v^2 (a.u.)	$E_{c.m.}$ (keV)	Basis set size	Charge transfer (10^{-18} cm^2)	$\sigma_t^{(1s)}$ (10^{-18} cm^2)	$\sigma_{st}^{(1s)}$ (10^{-18} cm^2)
0.7	14	35[a]	9.64		9.64
		34(tr)[b]	9.03	0.652	9.68
1.0	20	43	18.5	1.12	19.6
1.25	25	24[c]	23.3	1.07	24.4
		35[c]	23.6	1.36	25.0
1.5	30	43	25.8	2.99	28.8
		51	26.9	2.66	29.5
2.0	40	35[a]	27.2	3.99	31.2
		43	25.0	6.86	31.9
		34(tr)[b]	26.7	6.97	33.7
		51	27.6	5.59	33.2
3.0	60	24[a]	20.7	7.43	28.1
		43	19.5	9.63	29.2
		51	20.3	10.1	30.4
6.0	120	35[a]	5.83	10.8	16.6
		43	5.36	11.9	17.2
		51	5.36	13.7	19.1
8.0	160	43	5.05	9.30	14.35
12.0	240	43	0.646	7.68	8.32
		51	0.623	7.92	8.54
30.0	600	51	0.015	4.66	4.68

[a]Reference 23.
[b]Reference 25.
[c]Reference 24.

In Table II we present the results of the present electron stripping calculation at various velocities along with some previous results by Winter. This table illustrates the changes of the stripping cross section with basis set size. The composition of the basis sets are given in Table III. The 34(tr) refers to a triple-center atomic-state calculation in which a basis set was centered on the point midway between the nuclei in addition to functions centered at the two nuclei.[25] At each energy the results are listed in order of accuracy such that those we believe to be more accurate are lower in the column. The general trend is for the more accurate results to have larger stripping cross sections. For all velocities except that for which $v^2=6$ a.u. ($E_{c.m.}=120$ keV) the two most accurate cross sections are within 4% of each other. The point at $E_{c.m.}=120$ keV shows the poorest convergence. At this energy there is a relatively large increase of 11% in the stripping cross section in going from 43 to 51 functions. This is all due to an increase in the ionization cross section. The sensitivity of this cross section to basis set size is probably attributable to the fact that the peak of the ionization curve coincides with this energy. It is possible to use an even larger basis set here in order to obtain better convergence. However, considering the position of this point relative to the entire curve, as shown in Fig. 1, the improvement may not be worth the computational effort required. This particular point lies on a very steep part of the cross section curve and consequently a shift of even 10% would not change the curve significantly. It should be noted that we did not test for the effect of adding more *d* states to the basis set. The 3*d* orbital on the helium accounted for less than 2% of the total excitation probability at any energy, therefore it is assumed that the addition of more *d* functions will have little effect on the

TABLE III. Basis sets used in various Sturmian calculations.

	Proton		Helium		
Basis	*ns*	*np* ($m=0,1$)	*ns*	*np* ($m=0,1$)	*nd* ($m=0,1,2$)
24	1*s*, . . . , 6*s*	2*p*	1*s*, . . . , 6*s*	2*p*, . . . , 6*p*	
35	1*s*, . . . , 7*s*	2*p*, 3*p*	1*s*, . . . , 7*s*	2*p*, . . . , 8*p*	3*d*
43	1*s*, . . . , 8*s*	2*p*, . . . , 4*p*	1*s*, . . . , 12*s*	2*p*, . . . , 8*p*	3*d*
51	1*s*, . . . , 8*s*	2*p*, . . . , 8*p*	1*s*, . . . , 12*s*	2*p*, . . . , 8*p*	3*d*

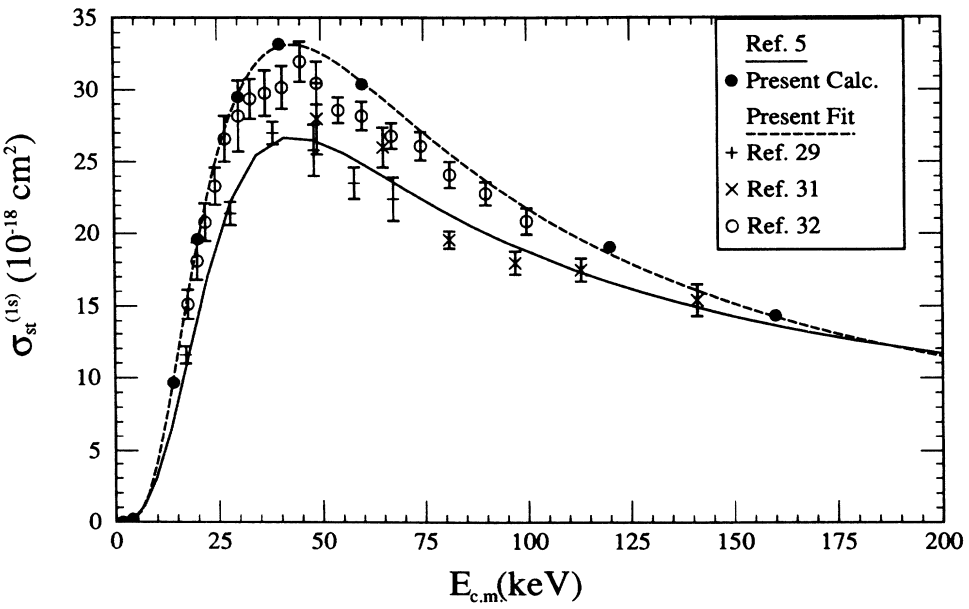

FIG. 2. Comparison of recent experimental stripping cross sections for the p-He^+ system with theoretical results at c.m. energies up to 200 keV. The theoretical data plotted are from the fit by Cohen (Ref. 5) and from the present calculations. The experimental data plotted are from Ref. 29, Ref. 31, and Ref. 32.

excitation cross sections. The effect of d functions on the proton has not been explored in this calculation. However, results from a previous investigation[22] showed that the d states contributed less than 1% to the electron transfer cross section. In Fig. 1 we have plotted some of the cross sections from Table II along with the analytic fit used by Cohen[36] and one set of experimental data which extends to energies above 200 keV. In Fig. 2 we have plotted other recent experimental results[29,31,32] along with the present theoretical results and Cohen's fit.

From Fig. 1 we can see that the present results lie about 10% above the Sturmian results obtained previously using smaller basis sets. Results from the triple-center calculations of Winter, however, agree quite well with the present values. When we compare our points with the analytic fit used by Cohen in reactivation calculations we notice first that the present Sturmian cross sections are nearly 25% larger at the peak than Cohen's fit of experimental data. However, at 200 keV they drop below this fit again and then finally converge with Cohen's cross sections at about 600 keV. As we shall see in Sec. IV, the result of this is that the overall probability of stripping a muon from the $1s$ state of $\alpha\mu$ is about the same whether we use Sturmian cross sections or Cohen's analytical fit. It should be pointed out that for energies above about 400 keV there is no experimental data available. In order to extend the analytic fit Cohen used the Born approximation for energies greater than 400 keV. It is well known that the Born approximation gives cross sections which are too large in the lower relative velocity range. This may be why the present calculations approach Cohen's curve from below as the energy is increased beyond about 200 keV.

The experimental data of Angel *et al.*[28] in Fig. 1 agree very well with the present results for c.m. energies above 200 keV. In Fig. 2 we can see that the lower energy experimental results along with their error bars span a significant range of possible cross sections at any one energy. This explains the uncertainty range of ±20% placed on Cohen's fit. It is encouraging to note that the

TABLE IV. Parameters for stripping and excitation cross sections in units of a_0^2 determined by a least-squares fit to Eqs. (16) and (17).

Equation	Transition	A_1	A_2	A_3	B_1	B_2
(14)	$1s$ (stripping) $v \leq 4$ a.u.	4.4	0.303	3.88	5.3	4.75
(14)	$1s$ (stripping) $v \geq 4$ a.u.	0.24	341.2	−2.4	7.28	1.16
(15)	$1s \rightarrow 2s$	0.586	2.64	7.19	0.01	1.11
(15)	$1s \rightarrow 2p$	35.4	1.31	5.69	155	3.30
(15)	$1s \rightarrow 3s$	0.111	4.26	−0.15	9.44	−0.83
(15)	$1s \rightarrow 3p$	0.28	0.14	8.4	4.44	2.97
(15)	$1s \rightarrow 3d$	0.025	4.49	−0.14	8.66	−0.68

most recent experimental data shown (Rinn *et al.*[32]) agree very well with the present results, particularly near the cross-section peak.

In order to use the present Sturmian cross sections over a continuous range of velocities so as to apply them to the reactivation calculation we have fitted the cross sections to functions similar to those used by Cohen. The stripping cross section was fitted to the following as a function of velocity:

$$\sigma_{\rm st}^{(1s)}=\frac{A_1 v^8}{(A_2+v^{B_1})(A_3+v^{B_2})} . \tag{16}$$

The $1s$-$2s$ and $1s$-$2p$ cross sections did not change appreciably from those used by Cohen, therefore we did not change the analytic fit. The $1s$-$3s$, $1s$-$3p$, and $1s$-$3d$ cross sections were fit to the following analytic function of velocity:

$$\sigma_{\rm ex}^{1s\rightarrow nl}=\frac{A_1 v^6}{(A_2+v^{B_1})(A_3+v^{B_2})} . \tag{17}$$

The parameters in Eqs. (16) and (17), as determined by a least-squares fit of the calculated results, are given in Table IV for each transition. These parameters give cross sections in atomic units if velocity is also given in atomic units where a velocity of 1 a.u. is equal to 2.1877×10^8 cm/s and a cross section of 1 a.u. is $a_0^2=2.8003\times10^{-17}$ cm^2.

IV. REACTIVATION CALCULATION

Reactivation refers to the process whereby a muon bound to an alpha particle $\alpha\mu$ emerging from the fusion reaction is stripped from the nucleus during passage through the medium (usually a mixture of D_2 and T_2) as a result of collisions with the various particles in its path. There are several dynamical processes which can occur during this series of collisions. The collision induced processes involved in reactivation are Auger transitions, Stark mixing, excitation and deexcitation, charge transfer, ionization, and slowing (stopping). For each of these processes one can calculate a rate using

$$\lambda=\rho\sigma v , \tag{18}$$

where ρ is the density of the medium, v the relative velocity, and σ the cross section for the process under consideration. Spontaneous deexcitations in which radiation is emitted also play an important role and so radiative deexcitation rates are also included. All of the various rates are used in a set of coupled differential equations which describe the kinetics of reactivation. We will define the reactivation coefficient as the probability that a bound muon has been stripped by the time $\alpha\mu$ has stopped in the medium by

$$R=P_{\rm st}(t=\infty)/\omega_s^0 , \tag{19}$$

where ω_s^0 is the probability that the muon will initially stick to the α particle after fusion and $P_{\rm st}$ is the stripping probability per fusion. The total stripping probability $P_{\rm st}$ is a time-dependent quantity determined by[10]

$$\frac{dP_{\rm st}(t)}{dt}=\sum_i \lambda_{\rm st}^{(i)}(v(t))P_i(t) , \tag{20}$$

where $\lambda_{\rm st}^{(i)}$ are the velocity-dependent stripping rates and $\{P_i\}$ are the time-dependent populations for the states $\{i\}$ of the $\alpha\mu$ ion. The time-dependent populations are determined by[10]

$$\frac{dP_i}{dt}=\Lambda_{\rm pop}^{(i)}-P_i\Lambda_{\rm depop}^{(i)} \tag{21}$$

with the initial conditions that $\{P_i(0)\}$ are the initial partial sticking fractions[37] and

$$\sum_i P_i(0)=\omega_s^0 . \tag{22}$$

The rate of populating state i ($\Lambda_{\rm pop}^{(i)}$) is given by

$$\Lambda_{\rm pop}^{(i)}=\sum_{i'\,(n_{i'}>n_i)}(\lambda_{\rm Au}^{(i'\rightarrow i)}+\lambda_{\rm ra}^{(i'\rightarrow i)}+\lambda_{\rm dex}^{(i'\rightarrow i)})P_{i'}+\sum_{i'\,(n_{i'}<n_i)}\lambda_{\rm ex}^{(i'\rightarrow i)}P_{i'}+\sum_{i'\,(n_{i'}=n_i)}\lambda_{\rm mix}^{(i'\rightarrow i)}P_{i'} \tag{23}$$

and the rate of depopulating state i is given by

$$\Lambda_{\rm depop}^{(i)}=\lambda_{\rm st}^{(i)}+\sum_{i'\,(n_{i'}<n_i)}(\lambda_{\rm Au}^{(i\rightarrow i')}+\lambda_{\rm ra}^{(i\rightarrow i')}+\lambda_{\rm dex}^{(i\rightarrow i')})+\sum_{i'\,(n_{i'}>n_i)}\lambda_{\rm ex}^{(i\rightarrow i')}+\sum_{i'\,(n_{i'}=n_i)}\lambda_{\rm mix}^{(i\rightarrow i')} , \tag{24}$$

where n_i refers to the principal quantum number of state i. The transition rates include Auger ($\lambda_{\rm Au}$), radiative ($\lambda_{\rm ra}$), collisional excitation ($\lambda_{\rm ex}$) and deexcitation ($\lambda_{\rm dex}$), Stark mixing ($\lambda_{\rm mix}$), and stripping ($\lambda_{\rm st}$) rates, and, except for $\lambda_{\rm ra}$, all of these rates are functionals of time. The functional dependence on the variable t results from the dependence of the rates on velocity according to Eq. (18), where the velocity appears explicitly and the cross section σ is itself a function of velocity. The dependence of velocity on time is determined by the equation

$$\frac{dE}{dt}=-\rho\sigma_s(v)v(t) , \tag{25}$$

where σ_s is the stopping cross section in units of area times energy, and ρ is the density of the medium. We will take the energy E to be that in the lab frame such that $v(t)=(2E/M_{\alpha\mu})^{1/2}$, where $M_{\alpha\mu}$ is the mass of $\alpha\mu$. The slowing down rate is independent of the target mass so results for a tritium target will be identical to those for a deuterium target. Consequently the results of this calculation will be independent of the ratio of D_2 to T_2 concentration in the medium.

In Sec. III we presented the results of our calculations of the cross sections in proton-He^+ collisions. In order to use these cross sections for $\alpha\mu$ one can simply assume a system of muonic atomic units in which the reduced mass of the muon-alpha system is equal to 1 muonic unit

(1 mu) of mass and the muonic bohr radius to 1 mu of length (a_μ). This is equivalent to the following scaling:

$$\sigma_\mu(v)=\sigma_e(v)\left[\frac{m_e}{m_\mu}\right]^2, \tag{26}$$

where m_e and m_μ are reduced masses and the subscripts e and μ refer to the electron and the muon, respectively. Taking into account the fact that the energy thresholds for various processes in the muonic system are quite different from those in the proton-He^+ system, Cohen has used the following scaling:[5]

$$\sigma_\mu(v)=\left[\frac{m_e}{m_\mu}\right]^2\frac{1}{(1+\epsilon)^2}[\sigma_e(v_1)-\epsilon^2\sigma_e(v_2)], \tag{27}$$

where $v_1=v/(1+\epsilon)$, $v_2=\epsilon v/(1+\epsilon)$, $\epsilon=2x-1-[(2x-1)^2-1]^{1/2}$, and x is equal to the ratio of collision energy to muon threshold energy. We have used Eq. (27) in the present calculations, although for the energies of interest Eq. (26) is adequate.

Scaled cross sections from the present Sturmian calculation have been used for $\lambda_{st}^{(1s)}$, $\lambda_{ex}^{(1s\to 2s)}$, $\lambda_{ex}^{(1s\to 2p)}$, $\lambda_{ex}^{(1s\to 3s)}$, $\lambda_{ex}^{(1s\to 3p)}$, and $\lambda_{ex}^{(1s\to 3d)}$. Stark mixing rates between the states $3s$, $3p$, and $3d$ were not assumed to be infinite but were calculated explicitly using the fixed field approximation of Leon and Bethe.[38] The Stark cross sections for $n=3$ do not have a large effect on the reactivation coefficient but will be important in a calculation of the x-ray yield. The Stark cross sections for $n=2$ and $n=3$ were fitted by the following analytical expression:

$$\sigma_{mix}^{(i\to f)}=a/v^b \tag{28}$$

Table V contains the values of the coefficients in Eq. (28) for the various Stark transitions indicated where the velocities and resulting cross sections will be in atomic units. For the remaining cross sections we used the following relationships:

$$\begin{aligned}
\sigma_{mix}^{(2p\to 2s)}&=\sigma_{mix}^{(2s\to 2p)}/3\ ,\\
\sigma_{mix}^{(3p\to 3s)}&=\sigma_{mix}^{(3s\to 3p)}/3\ ,\\
\sigma_{mix}^{(3d\to 3s)}&=\sigma_{mix}^{(3s\to 3d)}/5\ ,\\
\sigma_{mix}^{(3d\to 3p)}&=3\sigma_{mix}^{(3p\to 3d)}/5\ .
\end{aligned} \tag{29}$$

All other cross sections and rates are identical to those used by Cohen.[36]

In determining the error bars to be placed on the value of R we must first determine the error bars inherent in each of the values which are used in the calculation of R.

TABLE V. Parameters for the Stark cross sections in atomic units according to Eq. (28).

Transition	a	b
$2s\to 2p$	5.5×10^{-3}	1.8
$3s\to 3p$	2.37×10^{-2}	1.64
$3s\to 3d$	1.67×10^{-3}	2.00
$3p\to 3d$	1.1×10^{-2}	1.7

The two most important values are the stopping power and the stripping cross section from the $1s$ state. The accepted error bars for stopping are $\pm 10\%$. Based on the convergence of the stripping cross section in Table I and in Fig. 1 and the proximity to the latest experimental values we have assumed error bars of $\pm 4\%$ over the entire range of energies. Recall, however, that this estimation of error bars is valid for the p-He^+ system and does not take into account the error involved in using Eq. (26) to scale the results to the p-$\alpha\mu$ system. Recently we have estimated the error involved in such a scaling.[39] It was concluded that the error was significant only at velocities less than 2 a.u. We explicitly included the effect of this error and found that it increased R by less than 1%. The error in the excitation cross sections calculated for transitions from $1s$ to $2s$, $2p$, $3s$, $3p$, and $3d$ was found to be no more than $\pm 5\%$. The other cross sections are assigned error bars as follows: stripping (from $n>1$) $\pm 10\%$, excitation (from $n>1$) $\pm 10\%$, Stark mixing[14] $\pm 10\%$, and Auger[5] $\pm 50\%$. By performing numerical tests in which various cross sections were altered by the maximum error (as given above) we have determined error bars for the reactivation coefficient of $\pm 9\%$ at 1.2 LHD and $\pm 11\%$ at 0.05 LHD.

By considering the reactivation of the muon one obtains a lower probability that a muon will be lost to the catalytic cycle via sticking. The effective sticking factor which results is defined as

$$\omega_s^{eff}=(1-R)\omega_s^0\ . \tag{30}$$

Table VI contains values of the reactivation coefficient R, and the effective sticking fraction ω_s^{eff} as well as error bars for the present calculation and other recent calculations all as a function of the density given in units of liquid hydrogen density. From Table VI we can see that the present calculations give values for R very close to other recent theoretical values. In fact all of the results shown fall within the error we have given. The present results for R tend to be slightly smaller than the other recent work. We also indicate the approximate stopping time for the $\alpha\mu$ projectile which has an initial velocity of 5.83 a.u. (1.28×10^9 cm/s). Note that at a density of 10^{-4} LHD the stopping time is already about one fourth the lifetime of a muon (2.2×10^{-6} s). Thus densities of this order (or smaller) are not practical for MCF.

In Fig. 3 we compare our results for ω_s^{eff} with experimentally measured values from two different sources.[40,41] The experimental values agree with each other within the error bars only for densities between about 0.4 to 1.1 LHD. Above and below this range there is a serious discrepancy which raises a question about the density dependence of ω_s^{eff}. This discrepancy was a part of the motivation of the present work. The present results indicate a larger effective sticking than the experimental measurements for densities above 0.6 LHD. The data of Breunlich *et al.*[40] do not overlap the present results at any density. They do, however, exhibit a similar density dependence. The data of Jones *et al.*[41] overlap the present results only at densities from 0.2 to 0.6 LHD and indicate a much stronger density dependence than the

TABLE VI. The reactivation coefficient R and effective sticking fraction for $\alpha\mu$ with $\omega_s^0=0.886\%$ (Ref. 37).

Source	ρ (LHD)	R	ω_s^{eff} (%)	Stopping time (s)
This work	2.4	0.36±0.03	0.57±0.03	2×10^{-11}
	1.2	0.34±0.03	0.58±0.03	4×10^{-11}
	0.5	0.31±0.03	0.61±0.03	1×10^{-10}
	0.2	0.29±0.03	0.63±0.03	2×10^{-10}
	0.1	0.28±0.03	0.64±0.03	5×10^{-10}
	0.05	0.27±0.03	0.65±0.03	9×10^{-10}
	0.001	0.26±0.03	0.66±0.03	5×10^{-8}
	0.0001	0.21±0.03	0.70±0.03	5×10^{-7}
Ref. 7	1.2	0.36	0.57	
	0.1	0.30	0.62	
Ref. 14	1.2	0.35±0.05	0.58±0.05	
	0.05	0.29±0.05	0.63±0.05	
Ref. 6	1.2	0.35	0.58	
Ref. 12[a]	1.2	0.30	0.62	
	0.1	0.28	0.64	
Ref. 5	1.2	0.36±0.05	0.57±0.05	
	0.1	0.30±0.05	0.62±0.04	

[a]Stark mixing cross section used was $260.0/v^2$ in muonic units.

present or other theoretical results. Also shown are the theoretical results of Struensee and Cohen[14] with the margin or error indicated (dotted lines). It is interesting to note that the margin of error for the present results (dashed lines) lies entirely within their margin of error, although a slightly more pronounced density dependence is observed.

V. X-RAY TRANSITIONS

The intensity of x-ray transitions in $\alpha\mu$ is another quantity which can be measured experimentally and calculated along with R. According to the notation used previously[6,13] we define, for a transition x, the quantities γ_x to be the photon intensity per sticking event, $Y(x)$ to

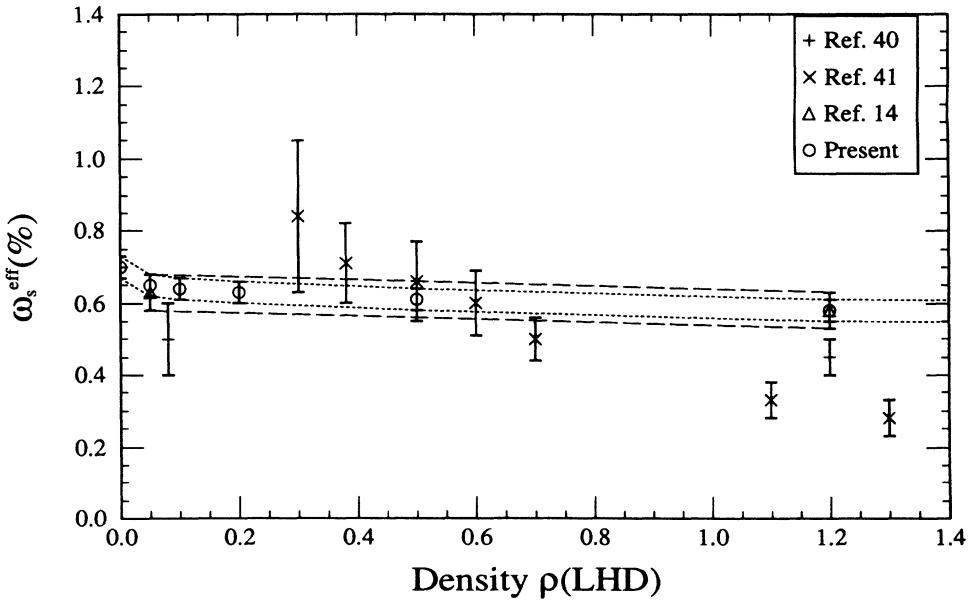

FIG. 3. Effective sticking factor vs density: theory and experiment. The theoretical data are bordered above and below by lines which enclose the margin of error. They correspond to results from Ref. 14 (dashed lines) and the present calculations (dotted lines). The experimental data plotted are from Breunlich *et al.* (Ref. 40) and from Jones *et al.* (Ref. 41).

be the intensity per fusion, and I_x to be the intensity per muon. These quantities are related to each other as follows

$$I_x = Y(x)\chi = \gamma_x \omega_s^0 \chi \ , \tag{31}$$

where χ is the average number of fusions per muon. The most useful quantity to compare with experiment is $Y(x)$.

We will consider only certain K-series and L-series transitions. The K series corresponds to the $n \rightarrow 1$ transitions and the L series to the $n \rightarrow 2$ transitions. The photon intensity per fusion for the $n' \rightarrow n$ transition is given by

$$Y(n' \rightarrow n) = \gamma_{n' \rightarrow n} \omega_s^0 \ , \tag{32}$$

where γ is calculated from

$$\frac{d\gamma_{n' \rightarrow n}}{dt} = \sum_{i' \, (n_{i'}=n')} \sum_{i \, (n_i=n)} \lambda_{\mathrm{ra}}^{(i' \rightarrow i)} P_{i'} \ . \tag{33}$$

In Table VII we compare our calculated photon intensities with other theoretical results and experimental data for the $K\alpha$ and $L\alpha$ transitions. For the other transitions in each series we compare the ratios of intensities to the α transition in that same series. The present result for $Y(K\alpha)$ agrees exactly with the most recent theoretical result available (Rafelski *et al.*[7]) at 1.2 LHD but their results indicate a stronger density dependence than do the present results. The other theoretical results listed in the table are 10–20% lower than the present at both high and low density.[6,13,14,42] The experimental values[3,4,43] for $Y(K\alpha)$ are all lower than the present calculated value. The present results for $Y(K\beta)$ agree well with those of Rafelski *et al.*, but are generally lower than the other theoretical results. The present results for $Y(K\gamma)$ are higher than all the other results listed in the table. The ratios of $Y(K\beta)$ and $Y(K\gamma)$ to $Y(K\alpha)$ are in excellent agreement with the experimental data of Bossy *et al.*[4] There are no experimental data available for the L-series transitions. The present calculated intensities for the $L\alpha$ and $L\beta$ transitions agree well with those of Cohen.[13]

VI. DISCUSSION AND CONCLUSIONS

Having completed the calculation of R as a function of density using results from an accurate stripping calculation we find that the values and trends in R, and consequently in ω_s^{eff}, do not differ significantly from the results of other recent theoretical work.[6,7,14] The primary difference between the present and previous theoretical results is the reduction in the margin of uncertainty claimed. From the outset we identified the uncertainty in the cross section for stripping from the $1s$ state $\sigma_{\mathrm{st}}^{(1s)}$ as the major source of uncertainty in R. We have achieved our goal of significantly lowering the uncertainty in R by calculating $\sigma_{\mathrm{st}}^{(1s)}$ using a coupled-state Sturmian method with a very large set of basis functions. The 9% uncertainty in R at 1.2 LHD can be approximately broken down as follows: 5% from the stopping cross section, 2% from the $\alpha\mu(1s)$ stripping cross section ($<1\%$ of which is from the use of scaling to convert to muonic cross sections), and 2% from the uncertainty in the other quantities involved in the multistep processes. At the lower density of 0.05 LHD there is essentially no contribution to R from the multistep processes and thus the 11% uncertainty at this density is entirely from the stopping cross section (8%) and the $\alpha\mu(1s)$ stripping cross section (3%).

Despite our lowering of the error bars on the reactivation coefficient it is still very difficult to draw any mean-

TABLE VII. Photon x-ray intensities per fusion for $\alpha\mu$ with $\omega_s^0 = 0.886\%$.

Source	$Y(K\alpha)$ ($\times 100$) 1.2 LHD	0.1 LHD	$Y(K\beta)/Y(K\alpha)$ 1.2 LHD	0.1 LHD	$Y(K\gamma)/Y(K\alpha)$ 1.2 LHD	0.1 LHD
			K series			
Present	0.30	0.35	0.081	0.124	0.020	0.040
Ref. 7	0.30	0.38	0.07	0.08[a]	0.012	
Ref. 14	0.27	0.32[b]				
Ref. 6	0.25	0.30	0.12	0.17	0.018	0.035
Ref. 13	0.25	0.30	0.12	0.19	0.019	0.038
Ref. 42	0.24	0.32	0.18	0.17	0.024	0.048
Experiments	1 LHD		1 LHD		1 LHD	
Ref. 3	0.049±0.04					
Ref. 43	0.21±0.05					
Ref. 4	0.19±0.05		≤0.08		0.020±0.013	
Source	$Y(L\alpha)$ ($\times 100$) 1.2 LHD	0.1 LHD	$Y(L\beta)/Y(L\alpha)$ 1.2 LHD	0.1 LHD		
			L series			
Present	0.023	0.052	0.17	0.18		
Ref. 13	0.023	0.042	0.13	0.17		

[a]Obtained from graph.
[b]Density of 0.05 LHD.

ingful conclusions concerning the experimental data. One could interpret the present results as partial confirmation of the data from 0.2 LHD to 0.6 LHD of Jones *et al.*,[41] even though these experiments exhibit much more density dependence. Above 0.6 LHD all of the experimental data shows lower effective sticking than theory predicts. Around liquid hydrogen density the experimental data is 20–40 % lower than theory predicts. Since the two sets of experimental data disagree with each other, there must be some errors made in at least one of the experiments or in the interpretation of raw data. We believe that theoretical results do not indicate which of the experiments is more likely to be correct.

The present experimental results on x-ray yields are also in substantial disagreement with theory at around 1 LHD. The experimental data of Bossy *et al.*[4] is about 30% lower than the present theory predicts. It is interesting to note that the data from most of the x-ray experiments are lower than the present theory by about the same amount (30%) as the data from the experiments on effective sticking are from theory at liquid hydrogen density. Because x-ray detection experiments are qualitatively different from neutron detection experiments we would not expect the systematic errors appearing in x-ray yield data to be the same as those in the effective sticking data. This sends a strong signal that the deviation from experiment may still be coming from the theoretical side. It is not obvious how an error in the reactivation calculations could bring about similar discrepancies in both x-ray yield and effective sticking. The process with the most uncertainty remaining in this calculation is the stopping cross section, which has an effect on the x-ray yield opposite to that on effective sticking.[7] Therefore, the present investigation points to initial sticking as a possible source of discrepancy which has the same effect on x-ray yield as on effective sticking.

Theoretical reactivation may still be in error if there exists an as yet unidentified aspect of the dynamics which is not being modeled properly, such as the stopping of $\alpha\mu$ in D_2-T_2. The stopping cross section is assumed to be equal to the stopping cross section of a proton in H_2 which is a reasonable assumption since the theoretical stopping cross section is dependent on projectile charge but independent of projectile or target mass. There is, however, some evidence that there may be some surprises in the dynamics of stopping in the condensed phase of D_2.[44]

Except for any possible new insights into the stopping cross section, as mentioned above, we believe there is little left to be done in the calculation of R. It is doubtful that the error in the stripping cross section can be significantly reduced. However, a further minor reduction of the error bars is possible by using realistic Coulomb trajectories in the calculation of $\sigma_{st}^{(1s)}$, which would eliminate the error caused by scaling. For a more accurate calculation of x-ray yields it would be helpful to calculate more accurate cross sections for the $n=2$ to 3 transition including the state-to-state cross sections for specific initial and final l quantum numbers.

ACKNOWLEDGMENTS

This work was supported by a grant from the Division of Advanced Energy Projects of the U.S. Department of Energy as well as a grant from the National Science Foundation. C.D.S. is grateful for support by the Division of Sponsored Research, University of Florida. T.G.W. has been supported by the U.S. Department of Energy, Office of Energy Research, Office of Basic Energy Sciences, Division of Chemical Sciences. We are also grateful to the North East Regional Data Center at the University of Florida for computer time.

[1]S. E. Jones, A. N. Anderson, A. J. Caffrey, C. DeW. Van Siclen, K. D. Watts, J. N. Bradbury, J. S. Cohen, P. A. M. Gram, M. Leon, H. R. Maltrud, and M. A. Paciotti, Phys. Rev. Lett. **56**, 588 (1986).

[2]W. H. Breunlich, M. Cargnelli, P. Kammel, J. Marton, N. Naegele, P. Pawlek, A. Scrinzi, J. Werner, J. Zmeskal, J. Bistirch, K. M. Crowe, M. Justice, J. Kurck, C. Petitjean, R. H. Sherman, H. Bossy, H. Daniel, F. J. Hartmann, W. Neumann, and G. Schmidt, Phys. Rev. Lett. **58**, 329 (1987).

[3]K. Nagamine, T. Matsuzaki, K. Ishida, Y. Hirata, Y. Watanabe, R. Kadono, Y. Miyake, K. Nishiyama, S. E. Jones, and H. R. Maltrud, Muon Cat. Fus. **1**, 137 (1987).

[4]H. Bossy, H. Daniel, F. J. Hartmann, W. Neumann, H. S. Plendl, G. Schmidt, T. von Egidy, W. H. Breunlich, M. Cargnelli, P. Kammel, J. Marton, N. Nagele, A. Scrinzi, J. Werner, J. Zmeskal, and C. Petitjean, Phys. Rev. Lett. **59**, 2864 (1987).

[5]J. S. Cohen, Phys. Rev. Lett. **58**, 1407 (1987).

[6]V. E. Markushin, Muon Cat. Fus. **3**, 395 (1988).

[7]H. E. Rafelski, B. Muller, J. Rafelski, D. Trautmann, and R. D. Viollier, Prog. Part. Nucl. Phys. **22**, 279 (1989).

[8]J. D. Jackson, Phys. Rev. **106**, 330 (1957).

[9]S. S. Gershtein, Yu. V. Petrov, L. I. Ponovarev, N. P. Popov, L. P. Presnyakov, and L. N. Somov, Zh. Eksp. Teor. Fiz. **80**, 1690 (1981) [Sov. Phys.—JETP **53**, 872 (1981)].

[10]L. Bracci and G. Fiorentini, Nucl. Phys. **A364**, 383 (1981).

[11]L. I. Men'shikov and L. I. Ponomarev, Pis'ma Zh. Eksp. Teor. Fiz. **41**, 511 (1985) [JETP Lett. **41**, 623 (1985)].

[12]H. Takahashi, Muon Cat. Fus. **1**, 237 (1987).

[13]J. S. Cohen, Muon Cat. Fus. **3**, 421 (1988).

[14]M. Struensee and J. S. Cohen, Phys. Rev. A **38**, 44 (1988).

[15]L. Wilets and D. F. Gallaher, Phys. Rev. **147**, 13 (1966).

[16]R. Shakeshaft, J. Phys. B **8**, 1114 (1975).

[17]R. Shakeshaft, Phys. Rev. A **18**, 1930 (1978).

[18]R. E. Olson, J. Phys. B **11**, L227 (1987).

[19]B. H. Bransden and C. J. Noble, J. Phys. B **14**, 1849 (1981).

[20]B. H. Bransden, C. J. Noble, and J. Chandler, J. Phys. B **16**, 4191 (1983).

[21]J. F. Reading, A. L. Ford, and R. L. Becker, J. Phys. B **15**, 625 (1982).

[22]T. G. Winter, Phys. Rev. A **25**, 697 (1982).

[23]T. G. Winter, Phys. Rev. A **33**, 3842 (1986).

[24]T. G. Winter, Phys. Rev. A **35**, 3799 (1987).

[25]T. G. Winter, Phys. Rev. A **37**, 4656 (1988).

[26]B. Peart, R. Grey, and K. T. Dolder, J. Phys. B **10**, 2675 (1977).

[27]G. C. Angel, E. C. Sewell, K. F. Dunn, and H. B. Gilbody, J. Phys. B **11**, L297 (1978).

[28]G. C. Angel, K. F. Dunn, E. C. Sewell, and H. B. Gilbody, J. Phys. B **11**, L49 (1978).
[29]B. Peart, K. Rinn, and K. Dolder, J. Phys. B **16**, 1461 (1983).
[30]K. Rinn, F. Melchert, and E. Salzborn, J. Phys. B **18**, 3783 (1985).
[31]M. F. Watts, K. F. Dunn, and H. B. Gilbody, J. Phys. B **19**, L355 (1986).
[32]K. Rinn, F. Melchert, K. Rink, and E. Salzborn, J. Phys. B **19**, 3717 (1986).
[33]H. H. Anderson and J. F. Ziegler, *Hydrogen Stopping Power and Ranges in All Elements* (Pergamon, New York, 1977).
[34]J. B. Delos, Rev. Mod. Phys. **53**, 287 (1981).
[35]Lovell and McElroy, Proc. R. Soc. London Ser. A **283**, 100 (1965).
[36]J. S. Cohen, Muon Cat. Fus. **3**, 499 (1988).
[37]S. E. Haywood, H. J. Monkhorst, and K. Szalewicz, Phys. Rev. A **37**, 3393 (1988).
[38]M. Leon and H. A. Bethe, Phys. Rev. **127**, 636 (1962).
[39]C. D. Stodden, H. J. Monkhorst, and K. Szalewicz, in *Muon-Catalyzed Fusion,* Proceedings of a Conference on Muon-Catalyzed Fusion, Sanibel Island, 1988, AIP Conf. Proc. No. 181, edited by S. E. Jones, J. Rafelski, and H. J. Monkhorst (AIP, New York, 1989).
[40]W. H. Breunlich, M. Cargnelli, P. Kammel, J. Marton, N. Naegele, P. Pawlek, A. Scrinzi, J. Werner, J. Zmeskal, J. Bistirch, K. M. Crowe, M. Justice, J. Kurck, C. Petitjean, R. H. Sherman, H. Bossy, H. Daniel, F. J. Hartmann, W. Neumann, G. Schmidt, and T. von Egidy, Muon Cat. Fus. **1**, 67 (1987).
[41]A. J. Caffrey, A. N. Anderson, C. DeW. Van Siclen, K. D. Watts, J. N. Bradbury, P. A. M. Gram, M. Leon, H. R. Maltrud, M. A. Pacioti, and S. E. Jones, Muon Cat. Fus. **1**, 54 (1987).
[42]H. Takahashi, Muon Cat. Fus. **3**, 453 (1988).
[43]F. J. Hartmann, H. Bossy, H. Daniel, T. von Egidy, W. Neumann, H. S. Plendl, W. Schott, P. Weisgerber, P. Ackerbauer, W. H. Breunlich, M. Cargnelli, M. Jeitler, P. Kammel, J. Marton, N. Nagele, A. Scrinzi, J. Werner, J. Zmeskal, C. Petitjean, J. Bistirlich, K. Crowe, M. Justice, and R. H. Sherman, Muon Cat. Fus. **2**, 53 (1988).
[44]P. Borgesen, Nucl. Instrum. Methods Phys. Res. B **12**, 73 (1985).